BioMetals **17:** 699–706, 2004.

Effects of surface hydrophobicity on the catalytic iron ion retention in the active site of two catechol 1,2-dioxygenase isoenzymes

Giovanna Di Nardo[1,*], Enrica Pessione[1], Maria Cavaletto[2], Laura Anfossi[3], Adriano Vanni[3], Fabrizio Briganti[4] & Carlo Giunta[1]

[1]*Dipartimento di Biologia Animale e dell'Uomo, Università di Torino, Via Accademia Albertina 13, 10123 Torino, Italy.* [2]*Dipartimento di Scienze e Tecnologie Avanzate, Università del Piemonte Orientale, C.so Borsalino 54, 15100 Alessandria, Italy.* [3]*Dipartimento di Chimica Analitica, Università di Torino, Via Pietro Giuria 5, 10126 Torino, Italy.* [4]*Dipartimento di Chimica, Università di Firenze, via della Lastruccia 3, 50019, Sesto Fiorentino, Firenze, Italy.* **Author for correspondence (Tel: 0039-011-6704645; Fax: 0039-011-6704692; E-mail: giovanna.dinardo@unito.it)*

Received 22 March 2004; Accepted 3 June 2004; Published online October 2004

Key words: apoenzymes, catalytic iron ion, catechol 1,2-dioxygenase, isoenzymes, superficial hydrophobicity

Abstract

The different behaviour of two isozymes (IsoA and IsoB) of catechol 1,2-dioxygenase (C1,2O) from *Acinetobacter radioresistens* S13 on a hydrophobic interaction, Phenyl-Sepharose chromatographic column, prompted us to investigate the role of superficial hydrophobicity on structural-functional aspects for such class of enzymes. The interaction of 8-anilino-1-naphtalenesulphonate (ANS), a fluorescent probe known to bind to hydrophobic sites in proteins, revealed that the two isoenzymes have a markedly different hydrophobicity degree although a similar number of hydrophobic superficial sites were estimated (2.65 for IsoA and 2.18 for IsoB). ANS is easily displaced by adding the substrates catechol or 3-methylcatechol to the adduct, suggesting that the binding sites are in the near surroundings of the catalytic clefts. The analysis of the hydropathy profiles and the possible superficial cavities allowed to recognize the most feasible region for ANS binding.

The lower hydrophobicity detected in the near surroundings of the catalytic pocket of IsoB supports its peculiarity to lose the catalytic metal ions more easily than IsoA. As previously suggested for other metalloenzymes, the presence of more hydrophilic and/or smaller residues near to the active site of IsoB is expected to increase the metal ligands mobility thus increasing the metal ion dissociation rate constants, estimated to be 0.078 h^{-1} and 0.670 h^{-1} for IsoA and IsoB respectively.

Abbreviations: C1,2O – catechol dioxygenase; ANS – 8-anilino-1-naphthalenesulphonate; PHO – phenol hydroxylase oxygenase

Introduction

Catechol 1,2 dioxygenase (EC 1.13.11.1) is a key-enzyme of the beta-ketoadipate pathway, the route used by most microorganisms to convert toxic aromatic compounds into intermediates of the TCA cycle (Ornston & Stanier 1966). It catalyzes the conversion of catechols, generated from different aromatic molecules, to cis,cis-muconates. Its catalytic pocket contains a mononuclear ferric iron coordinated to two tyrosine and two histidine residues (Briganti *et al.* 1998). Until now, different isoenzymatic forms of catechol 1,2-dioxygenase have been described: the two isoforms present in *Frateuria* sp. ANA-18 (Aoki *et al.* 1984), the three isozymes $\alpha\alpha$, $\beta\beta$, $\alpha\beta$ found in *P. arvilla* C-1 (Nakai *et al.* 1990), the two isozymes CDI_1 and CDI_2 from *A. lwoffii* K24 (Kim & Ha 1997), the four isozymes from *Arthrobacter* sp. BA-5-17

(Murakami *et al.* 1998) and the two isozymes from *Burkholderia* (Suzuki *et al.* 2002).

In previous papers (Briganti *et al.* 2000, Pessione *et al.* 2001) we reported the purification and the biochemical characterization of the two C1,2O isoenzymes from *A. radioresistens* S13. The two proteins, IsoA and IsoB, showed different molecular masses and amino-terminal sequences but very similar catalytic behaviours including K_m and K_{cat}, substrate specificities and intra/extra ratios against 3-methylcatechol. Their different genetic determinants (Pessione *et al.* 2001, Caposio *et al.* 2002) and the G+C % gene contents (unpublished results) suggest that the two isoenzymes found in *A. radioresistens* S13 should not be genetically related.

Although the 'in vitro' catalytic properties of the two isoenzymes are very similar, various differences in terms of structural parameters (temperature, pI and pH stability, amino acid sequence) suggested us to further investigate the possible effects of these features on enzymes functionality (Briganti *et al.* 2000, Pessione *et al.* 2001). In particular, we analyzed the differences in superficial hydrophobicity by studying the interactions with the fluorescent probe ANS and their effects on the kinetics of catalytic iron ion removal and uptake, evidencing structural and functional divergences between the two isoenzymes.

Materials and methods

Bacterial strain, culture conditions, enzymes purification and identification

The *Acinetobacter radioresistens* S13 strain was maintained and cultured as previously referred (Briganti *et al.* 1997) and the isoenzymes were purified as described by Briganti *et al.* (2000).

A further purification step was added: a Phenyl-Sepharose-FPLC (Pharmacia Biotech) chromatography, previously equilibrated with 0.050 M Hepes/NaOH pH 7 + 0.5 M Na_2SO_4. An ionic strength decreasing gradient was applied in the range 0.5–0 M Na_2SO_4.

The identification of the two isoenzymes was performed determining the first 20 aminoacids using an Applied Biosystems 470A gas-phase sequencer (USA), equipped with an on-line model 120A phenylthiohydantoin (PHT) derivatives analyzer. The electrophoretic band corresponding to C1,2O was blotted into an Immobilon P membrane (Millipore) and then cut for use in the analyzer.

Protein determination and enzyme assay

The protein concentration and the enzymes activity were determined using a DU70 spectrophotometer (Beckman). The previously determined molar extinction coefficients at 280 nm and 430 nm were utilized for protein and metal content estimations (Briganti *et al.* 2000).

The ionic strength effect on catalysis was evaluated incubating the proteins ($1 \cdot 10^{-2}$ μM for each test) for 5 min in a Hepes/NaOH pH 7 buffer in the concentration range 0.010–0.50 M (corresponding to an ionic strength range 0.004-0.2 M) and then measuring the activity. The C1,2O activity was spectrophotometrically monitored (DU70, Beckman), following the formation of *cis,cis*-muconic acid at 260 nm (ε_{260} = 16 000 M^{-1} cm^{-1}).

Spectrofluorimetric measurement

Protein superficial hydrophobicity was investigated using a spectrofluorimetric assay with 1-anilinonaphtalene-8-sulphonate (ANS) as a probe for hydrophobic sites. The estimation of hydrophobic pockets number was made by the method described by Cardamone and Puri (1992).

The ANS-proteins interaction was analysed using a LS50 B-Perkin Elmer fluorescence spectrophotometer. The excitation wavelength was 388 nm and the emission spectrum was recorded between 400 and 700 nm. The spectral bandwidth used was 2 nm and the scan speed was 150 nm/min. Each spectrum was the result of 3 accumulation scans.

A calibration factor for our proteins was determined in order to relate the maximal change in fluorescence intensity per ANS (μM) bound to the protein. A fixed quantity of ANS (3 μM) was incubated with increasing concentrations of C1,2Os ranging from 0.3 to 30 μM. A double-reciprocal plot of fluorescence intensity *versus* protein concentration allowed to calculate the calibration factor from the intercept on the ordinate axis extrapolation, corrected for the protein concentration according to Cardamone and Puri (1992):

$$1/F = a/c + 1/\Delta F_{max}$$

$$\Delta F_{max} = \text{calibration factor} \cdot c$$

where F is the fluorescence intensity (arbitrary units), a is the slope, c is the concentration of the protein, ΔF_{max} is the maximal fluorescence increase observed, due to the saturation of all ANS binding sites.

A fixed quantity of each isozyme (3 μM) was incubated with increasing concentrations of ANS ranging from 3 to 100 μM, in a quartz optical cell and in a total volume of 3 ml (path-length 10 mm). Fluorescence measurement was recorded at 25 °C after 1 min; the delay was necessary to obtain a constant fluorescence signal. ANS concentrations lower than 50 μM were used because at higher concentrations the fluorescence signal was quenched.

The contribution of ANS to the fluorescence spectra was subtracted and data were elaborated by standard non-linear regression method using Microcal ORIGIN Software.

A Scatchard analysis was performed to calculate the binding constants k_b and the number of ANS-binding sites n:

$$B/F = -1/k_b B + n/k_b$$

where B is the concentration of bound ANS, and F the concentration of free ANS. Catechol and 3-methylcatechol, in a concentration range 0.5–100 μM, were used for ANS displacement experiments.

Sequence and structure analysis

Multiple sequence alignments were performed using the ClustalX program available on the NCBI server (Thompson *et al.* 1994) and the hydropathy profiles were determined using the method described by Black and Mould (1991).

The accessible molecular surfaces from the PDB structure of ADP1 (PDB code: 1DLT) were calculated using the Surface Racer 1.2 software (Tsodikov *et al.* 2002).

Apoenzymes preparation and reactivation

Metal removal experiments were performed using a cationic exchanger resin Amberlite IRC 50 functionalized with carboxylic groups (Sigma). The resin was washed in sequence with 3 volumes of 0.1 M EDTA, 0.1 M hydrochloric acid and milli-Q water. The resin was then swollen in 0.050 M Tris-SO_4 buffer pH 8. The buffer solution was finally removed and the wet resin stored at 4 °C.

To remove the active metal ions from the enzymes the incubation mixture (30 mg/ml of resin with 0.2 mg/ml enzyme, total volume 1 ml, in a buffer solution of 0.050 M Tris-SO_4 pH 8.0) was continuously stirred at 100 rpm, 4 °C up to 55–60 h and the activity was measured every 30 min. The apoenzyme was recovered by centrifugation.

The results were fitted to the pseudo-first order equation:

$$S = S_{\dot{0}}\, e^{-kremt} + b$$

where S is the specific activity, S_0 represents the difference between the initial specific activity and b, where b is the residual specific activity, k_{rem} represents the dissociation rate constant of the complex iron-enzyme in the presence of the resin and t the time (Ashmore 1979).

The apoenzymes were reactivated upon addition of different amounts of $(Fe)_2(SO_4)_3$ to estimate the proper Fe(III)/protein ratio to obtain the maximal enzyme reactivation. The activity was monitored after five minutes from the protein-catechol mixing to exclude possible interferences at 260 nm due to free iron-catechol complexes formation. The substrate was added in a large excess (80 μM) to ensure the saturation of enzyme catalytic sites.

Atomic absorption spectroscopy

The iron content was estimated during the metal removal processes. Measurements were carried out by electrothermal AAS using a Perkin Elmer 5000 spectrophotometer (electrically heated furnace: HGA 400, sampler AS 40). Each enzyme solution was diluted 1:10 in a HNO_3 0.2 % solution to obtain an iron concentration of about 20–30 ppb and then measured. A calibration curve was prepared by diluting an iron standard solution (Merck) to concentrations between 5 and 50 ppb in a 0.2% HNO_3 solution and measuring them in order to correlate the signal to iron concentration.

Thermal denaturation spectrometry.

An Ultrospec 2000 (Pharmacia Biotech) spectrophotometer was used to detect changes in the typical tyrosinate to iron charge transfer band (maximum at 430 nm) in the visible region during thermal denaturation in the temperature range (17–60 °C). The enzyme concentration was 30 μM.

Results and discussion

During the purification procedures IsoA and IsoB can be easily separated using a Phenyl-Sepharose chromatography: IsoB is not retained by the column in a Hepes 0.050 M pH 7 and 0.5 M Na_2SO_4 buffer, whereas IsoA is released only in the absence of

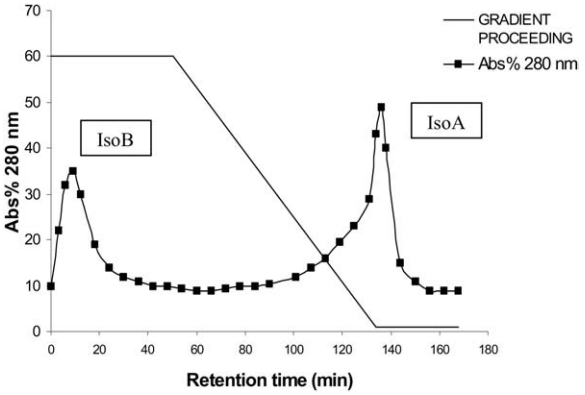

Figure 1. Phenyl-Sepharose chromatography pattern for an IsoA and IsoB mixture. The Na_2SO_4 salt gradient is also shown.

Na_2SO_4, thus displaying a more hydrophobic nature (Figure 1).

The comparison of their sequences (Caposio *et al.* 2002) (access number on the NCBI server: AF380158.1 for IsoA; AF182166.2 for IsoB) shows that the identity of the two isozymes is 48.4%. In particular the different proline (6.37% in IsoA and 3.92% in IsoB) and also asparagine (5.73% in IsoA and 3.92% in IsoB) contents, two residues known to destabilize the helix structure, suggest some divergences in folding and conformation of the two proteins. No significant differences are present in the total hydrophobic aminoacid content (38.8% for IsoA and 38.6% for IsoB) to explain the differential behaviour of the two isozymes interacting with the Phenyl-Sepharose resin. These are probably owed to a dissimilar superficial polarity of the two C1,2Os also supported by the observed effects of ionic strength on the catalytic activities of IsoA and IsoB. Indeed IsoA displays the highest activity at ionic strength of 0.012 M, whereas IsoB reaches its maximal activity at 0.040 M suggesting a different degree and distribution of electrostatic interactions with the substrate molecules or differential conformations induced by the changes in ionic strength.

These observations prompted us to investigate the surface hydrophobicity using spectrofluorimetric experiments with the fluorescent probe ANS since its quantum yield is known to considerably increase upon binding to superficial hydrophobic pockets of proteins (Brand & Gohlke 1972). The fluorescence intensities of different concentrations of ANS, in the absence and in the presence of the two C1,2O isozymes, were determined. The fluorescence increase was larger when IsoA was added to ANS (Figure 2a). Since the ANS

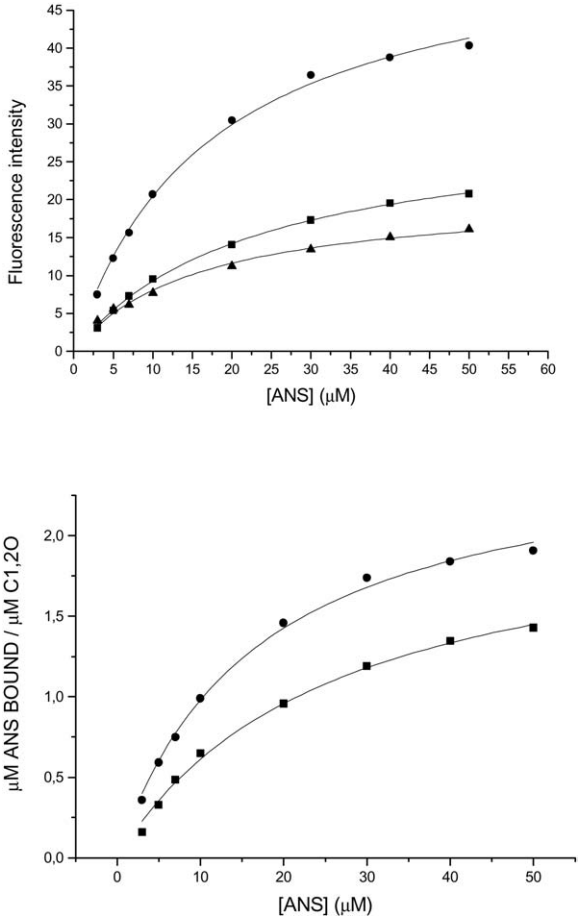

Figure 2. (a) ANS fluorescence intensity in the absence (▲) or in the presence of IsoA (●) and IsoB (■). b) Ratios of bound [ANS] per [C1,2O] as a function of total [ANS] obtained by the normalized curves of ANS fluorescence in the presence of IsoA (●) and IsoB (■) as reported in Materials and methods.

fluorescence yield is inversely proportional to the presence of water molecules, it was possible to realize that IsoA possesses either a larger number of ANS-binding sites or more hydrophobic sites than IsoB. The calibration factor, which represents the maximal fluorescence increase due to the interaction of 1 μM ANS with 1 μM enzyme was determined to quantify the number of ANS bound hydrophobic sites for the two proteins. The results obtained were 19.5 $\pm$ 1.2 arbitrary units/μM for IsoA and 10.8 $\pm$ 0.9 arbitrary units/μM for IsoB. The binding curves were normalized to the calibration factor and to the protein concentration, then a hyperbolic fitting was performed (Figure 2b). On the basis of the Scatchard analysis, the binding constants for the enzyme-ANS complex were estimated to be 16.6 $\pm$ 1.2 μM^{-1} for IsoA

and 25.9 ± 2.6 μM^{-1} for IsoB and the deduced ANS-binding sites were 2.65 ± 0.07 for IsoA and 2.18 ± 0.11 for IsoB. These results suggest that the different ANS fluorescence yields are not due to a substantial difference in ANS-binding sites number, but rather to their diverse hydrophobicity degree. This conclusion is also supported by the different blue shift in the maximal emission wavelength observed when the two isoenzymes are incubated with the probe: a larger blue shift has been observed for IsoA (from 515 nm to 478 nm) than for IsoB (from 515 nm to 487 nm).

When catechol (the physiological substrate) or 3-methylcatechol were added to the IsoA-ANS or IsoB-ANS adducts under saturating concentrations a sudden decrease of fluorescence, back to the original value of unbound ANS, was observed. This observation indicates that the ANS molecules are displaced by the substrates from their binding sites and that these sites are in the near surroundings of the active cavites (ANS is too bulky to enter the catalytic cavity itself). Such observation is also supported by kinetics studies on the inhibitory effects of ANS on both isoenzymes. IsoA and IsoB showed activity decreases of 31.4 ± 4.1%, and 36.8 ± 2.3% respectively on the activity of the two C1,2Os when ANS was added to the reaction mixture, at the same concentration of catechol (20 μM). A titration experiment performed by changing the substrate concentration to monitor the fluorescence changes was not feasible because the substrate was quickly converted by the enzyme allowing the ANS to bind again. The observed decrease of fluorescence signal back to the value of ANS-protein complex formation proves such deduction. A possible effect of fluorescence quenching, due to a conformational change of the proteins interacting with the substrate, was excluded since it is known that no conformational changes occur upon substrate binding to catechol dioxygenases (Vetting & Ohlendorf 2000).

Vetting and Ohlendorf (2000) suggested that some hydrophobic regions, found in C1,2O from *Acinetobacter* sp. ADP1, could be involved in the binding to other enzymes of the same catabolic pathway, thus accelerating the reaction by passing the product from one enzyme to the next. IsoA, which is the only C1,2O isozyme induced in the presence of phenol (Pessione *et al.* 2001), often co-elutes, in the Phenyl-Sepharose purification step, with phenol hydroxylase, the enzyme converting phenol into catechol, the catalytic subunit of which (PHO) is strongly hydrophobic (Divari *et al.* 2003). Therefore, the function of part of the hydrophobic domains could be their interaction with PHO, which is also a soluble protein (Giuffrida *et al.* 2001, Pessione *et al.* 2002). The observed larger superficial hydrophobicity of IsoA substantiates its tight association with phenol hydroxylase. In Figure 3 are reported the hydropathy profiles of IsoA and IsoB compared to C1,2O from *Acinetobacter calcoaceticus* sp. ADP1 (ADP1 hereafter). Their comparison reveals an almost total superimposition between IsoA and ADP1 whereas a few more hydrophilic regions appear to be present in IsoB in the regions surrounding residues 95, 130, 140-150, 240-250, 270-280 and 295-310. This is in accordance to the different percentage of sequence identities between IsoA and ADP1 (83%) and IsoB and ADP1 (48%).

The program Surface Racer 1.2 was utilized to calculate the accessible molecular surfaces and to analyze the superficial cavities in the crystal structure of ADP1 (PDB code 1DLM) (Tsodikov *et al.*, 2002). The analysis revealed the presence of a few cavities suitable for ANS binding, but only the region surrounding residue 305 showed hydrophilic substitutions capable to support the observed lower ANS affinities for IsoB. This corresponds to an external region on the side edge of the long cleft surrounding the active cavity composing the last C-terminal β-strand.

The fluorescence experiments performed in the presence of enzyme substrates support this hypothesis. From hydropathy profiles (Figure 2) it can also be noted that some regions (residues 30-50 and 180-195) are slightly more hydrophobic in IsoB than in IsoA and ADP1. Nevertheless, these regions, corresponding to α-helix 2 and β-sheet G respectively, are far-away from the active site cleft.

The sequence alignment between IsoA and ADP1 (83% identity) indicates that the region of IsoA including aminoacids 20-100 (the 'helical zipper' linker domain), a strongly hydrophobic site which binds phospholipids, is maintained in IsoA. In particular, the residues 30, 33, 45, 55, 61, 62, 65, 74, 78, 80 and 221 (ADP1 numbering), known to directly interact with the phospholipids in ADP1, are essentially conserved. The sequence identity between IsoB and ADP1 is lower (48%). Nevertheless most residues involved in phospholipid binding are substituted with homologous amino acids (Figure 3). For this reason the different superficial hydrophobicity observed between IsoA and IsoB cannot be attributable to differences in this region.

The most probable consequence of a more hydrophilic C-terminal in C1,2O is a higher mobility of its

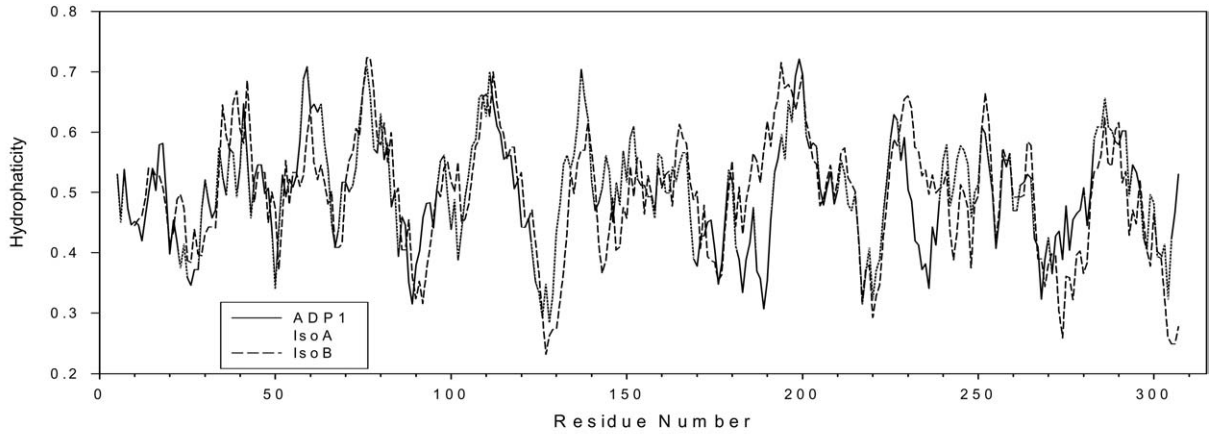


```
                1       10        20        30        40        50        60        70        80        90       100
ADP1       ---MEVKIFNT DV DFLRVASGLE EGG--NPRVK IIHRVLSDLYKAIEDLNITSDEYWAGVAYLN LGAN EAGLLSPGLGFDHYLDMRMDAEDAALGIENATPRTI
ISOA       MTAANVKILNTEEV NFINLLSGLE EGG--NPRIK IIHRVVSDLFKSIEDLEITSDEYWAAIAYLN LGTSHEAGLLSPGLGFDHFLDMRMDAIDAALGIDNPTPRTI
ISOB       --------MNR  IDALVK MN-VDTAKGPVDERI  VVVRLLGDLF AIEDLDI PSEVWKGLEYLTDAG ANELGLLAAGLGLEHYLDLRADEADAKAGITGGTPRTI
               110       120       130       140       150       160       170       180       190       200       210
ADP1       EGPLYVAGAPESVGYARMDDGSDPN-GHTLILHGTIFDADGKPLPNAKVEIWHANTKGFYSHFDPTGE  AFNMRRSIITDENG YRVRTILPAGYGCPPEGPT  LLN
ISOA       EGPLYVAGAPVS GFARMDDGSDPN-GHTLILHGTIYNADG PIPNA VEIWHANTKGFYSHFDPTGE TPFNMRRTIMTDA GHYRV TILPSGYGCPPNGPT  LLN
ISOB       EGPLYVAGAPESVGFARMDDGSESDKVDTLIIEGTVTDTEGNIIEGAKVEVWHANSLGNYSFFDKS-- SDFNLRRTILTDVNGKYVALTTMPVGYGCPPEGTT ALLNK
               220       230       240       250       260       270       280       290       300       310
ADP1       LGRHGNRPAHIHYFVSADGHRKLTT INVAGDPYTYDDFAYATREGLVVDAVEHTDPEAIKANDVEGPFAEMVFDLKLTRLVDGVDN VVDRPRLAV
ISOA       LGRHGNRPAHIHFFVSADGYRKLTT INVAGDPYTYDDFAFATREGLVVEAIEHTDPATS RNGVEGPFAEMVFDLKLSRLVDGVDN VVDRPRL A
ISOB       LGRHGNRPSHVHYFVSAPGYRKLTT FNIEGDEYLWDDFAFATRDGLVATATDVTDEAEIARRELDKPFKHITFNVELVKEAEAAPSSEVERRRASA
```

Figure 3. Hydropathy diagrams of ADP1 (solid line), IsoA (dotted line) and IsoB (dashed line) (Black& Mould, 1991) and aminoacid sequences alignment of the C1,2O from *Acinetobacter calcoaceticus* ADP1 (ADP1) and the two isozymes (IsoA and IsoB) from *Acinetobacter radioresistens* S13.

backbone and side chains, which could strongly influence both the ANS surface binding and the metal ion release from the active site.

Since it was previously observed that IsoB loses the catalytic iron ions more easily than IsoA (Briganti *et al.*, 2000), experiments of metal ion removal from the catalytic pockets of the two C1,2Os and reactivation of apo-enzymes by the addition of iron (III) were performed in order to understand if the different hydrophobicity of the regions surrounding the catalytic pockets could influence the metal ion-protein affinity.

Figure 4a shows that IsoA loses its activity very slowly, whereas IsoB undergoes a rapid loss of activity during the first three hours. The atomic absorption experiments demonstrate that the loss of activity is linearly proportional to the iron ion removal (Figure 4a).

The dissociation rate constants for the iron-enzyme complex in the presence of the chelator resin (k_{rem}) were estimated to be 0.078 ± 0.008 h^{-1} for IsoA and 0.670 ± 0.097 h^{-1} for IsoB, revealing that the catalytic metal ion is more strongly retained by the IsoA enzyme. The observed differences in metal dissociation constants cannot be related to differences in the metal ligands since the residues involved in the iron ion coordination to the proteins are conserved among the C1,2O family (Figure 3). They are Tyr168, Tyr204, His228 and His230 for IsoA; Tyr162, Tyr196, His220 and His222 for IsoB.

Both apoforms were immediately reactivated after the addition of iron(III) as sulphate salt (Figure 4b). The maximal activity was obtained in both cases by adding Fe(III) in a molar ratio Fe/protein of 20:1. Under these conditions IsoB was reactivated up to 80% of the original activity, whereas the activity of IsoA could be restored to only about 50%. These data suggest a different behaviour and ability of the two apoenzymes to uptake the iron ion. The longer time necessary to obtain the apoform of IsoA, compared to the IsoB apoform, could be due to a more buried and rigid iron ion

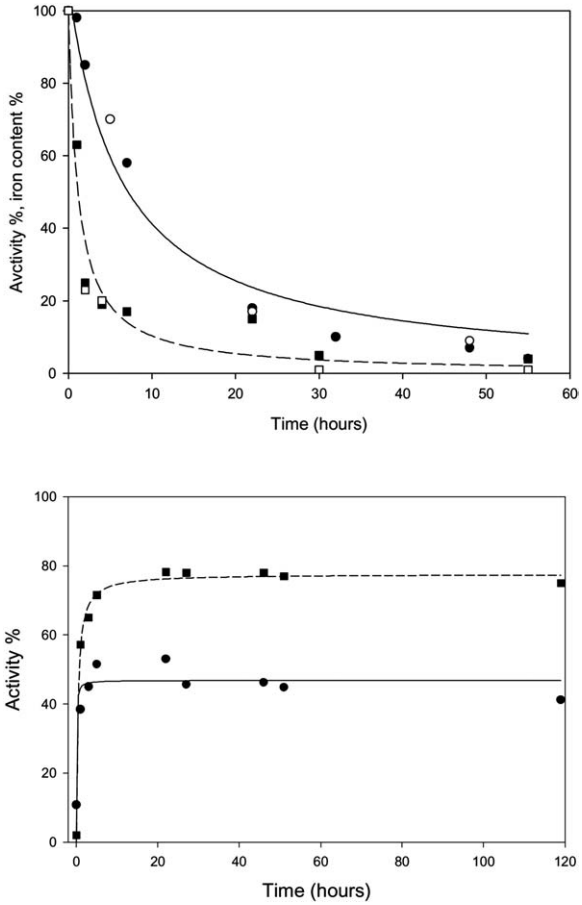

Figure 4. (a) Residual activity versus time of IsoA (● solid line) and IsoB (■ dotted line) during metal displacement. The white symbols (○ for IsoA and □ for IsoB) represent the iron content % of the enzymes. (b) Activity during the apoenzymes reactivation processes. Each point represents the average of five different experiments.

environment resulting in a larger and possibly irreversible loss of the IsoA structure upon metal ion removal. Further experiments need to be performed to understand the process and try to optimize the reactivation of apo-enzyme IsoA.

Nevertheless the differences in the iron ion release rates from the catalytic pockets are consistent with the different degree of hydrophobicity observed: IsoB loses its catalytic iron ion more easily than IsoA because its active sites regions are more exposed to the solvent environment than those of IsoA. On the other hand the higher superficial hydrophobicity of IsoA could have structural relations with its ability to bind the iron(III) stronger than IsoB. As previously reported, in the case of site directed mutagenesis experiments on Zn(II) containing human carbonic anhydrase II, the metal ion dissociation rate constants increase when smaller and/or more hydrophilic residues are substituted in the near surroundings of the metal ligands. Such substitutions produce an increase in the mobility of metal ions ligands facilitating their exchange with the solvent (Hunt *et al.* 1999). For IsoB it can be observed that Ala223 flanking the His224 ligand is substituted with a more hydrophilic Serine and Phe163 is changed into Asparagine. These substitutions could justify the observed differences in metal ion dissociation rate constants.

Further evidences supporting these observations come from thermal denaturation experiments followed monitoring the changes of the visible spectra absorbance maximum at about 430 nm (charge transfer transition tyrosine ligands → iron (III)) of both C1,2Os, in the temperature range 17–60 °C. Although the catalytic pockets of the two C1,2O isozymes show good stabilities at high temperature, appreciable changes regarding the active sites take place above 42 °C for IsoB and above 47 °C for IsoA accompanied by a consistent loss of activity for both isozymes. The higher lability of IsoB could be justified by a more solvent exposed conformation of its active site regions as suggested above.

It has been observed that the structural differences regarding the active cavity domains of the two C1,2Os have no effects on the catalytic parameters and substrate specificity (Briganti *et al.* 2000), but the 'in vivo' functionality of the two isozymes could sensibly differ since the present study demonstrates that it is strongly modulated by temperature, ionic strength, and hydrophobic interactions.

Experiments of crystallization to solve the molecular structure of IsoB, the primary sequence identity of which is only 48% of that of ADP1, are currently undergoing to definitely prove these observations.

Acknowledgements

This work was supported by grants from CIB (Consorzio Italiano Biotecnologie). We thank Dr. Leila Oddenino for generous help in apo-proteins preparation.

References

Aoki K, Konohana T, Shinke R, Nishira H. 1984 Two catechol 1,2-dioxygenase from an aniline-assimilating bacterium, *Frateuria species* ANA-18. *Agric Biol Chem* **48**, 2097–2104.

Ashmore PG. 1979 Principles of reaction kinetics Revised 2nd edition. London: The Chemical Society

Black SD, Mould DR. 1991 Development of hydrophobicity parameters to analyze proteins which bear post- or cotranslational modifications. *Anal Biochem* **193**, 72–82.

Brand L. Gohlke JR. 1972 Fluorescence probes for structure. *Annu Rev Biochem* **41**, 843–868.

Briganti F, Pessione E, Giunta C, Scozzafava A. 1997 Purification, biochemical properties and substrate specificity of a catechol 1,2-dioxygenase from a phenol degrading *Acinetobacter radioresistens*. *FEBS Lett* **416**, 61–64.

Briganti F, Mangani S, Pedocchi L, Scozzafava A, Golovleva LA, Jadan AP, Solyanikova IP 1998 XAS characterization of the active sites of novel intradiol ring-cleaving dioxygenases: hydroxyquinol and chlorocatechol dioxygenases. *FEBS Lett* **433**, 58–62.

Briganti F, Pessione E, Giunta C, Mazzoli R, Scozzafava A. 2000 Purification and catalytic properties of two catechol 1,2-dioxygenase isozymes from benzoate-grown cells of *Acinetobacter radioresistens. J Protein Chem* **19**, 709–716.

Caposio P, Pessione E, Giuffrida MG, Conti A, Landolfo S, Giunta C, Gribaudo G. 2002 Cloning and characterization of two catechol 1,2-dioxygenase genes from *Acinetobacter radioresistens* S13. *Res Microbiol* **153**, 69–74.

Cardamone M, Puri NK. 1992 Spectrofluorimetric assessment of the surface hydrophobicity of proteins. *Biochem J* **282**, 589–593.

Divari S, Valetti F, Caposio P, Pessione E, Cavaletto M, Griva E, Gribaudo G, Gilardi G, Giunta C. 2003 The oxygenase component of phenol hydroxylase from Acinetobacter radioresistens S13. *Eur J Biochem* **270**, 2244–2253.

Giuffrida MG, Pessione E, Mazzoli R, Dellavalle G, Barello C, Conti A, Giunta C. 2001 Media containing aromatic compounds induce peculiar proteins in Acinetobacter radioresistens, as revealed by proteome analysis. *Electrophoresis* **22**, 1705–1711.

Hunt JA, Ahmed M, Fierke CA. 1999 Metal binding specificity in carbonic anhydrase is influenced by conserved hydrophobic core residues. *Biochemistry* **38**, 9054–9062.

Kim SI, Kweon SM, Kim S, Ha, KS 1997 Peptide mapping and amino acid sequencing of two catechol 1,2-dioxygenases (CD I1 and CD I2) from *Acinetobacter lwoffii* K24. *Mol. Cells* **31**, 635–640.

Murakami S, Wang CL, Naito A, Shinke R, Aoki, K 1998. Purification and characterization of four catechol 1,2-dioxygenase isozymes from the benzamide-assimilating bacterium *Arthrobacter species* BA-5-17. *Microbiol Res* **153**, 163–171.

Nakai C, Horiike K, Kuramitsu S, Kagamiyama H, Nozaki M. 1990. Three isozymes of catechol 1,2-dioxygenase (pyrocatechase), alpha alpha, alpha beta, and beta beta, from *Pseudomonas arvilla* C-1. *J Biol Chem* **265**, 660–665.

Ornston LN, Stanier RY 1966. The conversion of catechol and protocatechuate to beta-etoadipate by *Pseudomonas putida. J Biol Chem* **241**, 3776–3786.

Pessione E, Giuffrida MG, Mazzoli R, Caposio P, Landolfo S, Conti A, Giunta C, Gribaudo G. 2001. The catechol 1,2 dioxygenase system of *Acinetobacter radioresistens*: isoenzymes, inductors and gene localisation. *Biol Chem* **382**, 1253–1261.

Pessione E, Giuffrida MG, Prunotto L, Barello C, Mazzoli R, Fortunato D, Conti A, Giunta C. 2003 Membrane proteome of Acinetobacter radioresistens S13 during aromatic exposure. *Proteomics* **3**, 1070–1076.

Suzuki M, Hayakawa T, Shaw JP, Rekik M, Harayama S. 1991 Primary structure of xylene monooxygenase: similarities to and differences from the alkane hydroxylation system. *J Bacteriol* **173**, 1690–1695.

Thompson JD, Higgins DG, Gibson TJ. 1994 CLUSTAL W: improving the sensitivity of progressive multiple sequence alignment through sequence weighting, position-specific gap penalties and weight matrix choice. *Nucleic Acids Re* **22**, 4673–4680.

Tsodikov OV, Record MT Jr, Sergeev YV. 2002 Novel computer program for fast exact calculation of accessible and molecular surface areas and average surface curvature. *J Comput Chem* **23**, 600–609.

Vetting MW, Ohlendorf DH 2000 The 1.8 A crystal structure of catechol 1,2-dioxygenase reveals a novel hydrophobic helical zipper as a subunit linker. *Structure Fold Des* **8**, 429–440.